Experimental and Theoretical Examination of C−CN Bond Activation of Benzonitrile Using Zerovalent Nickel

Tülay A. Ateşin, Ting Li, Sébastien Lachaize, Juventino J. García, and William D. Jones*

Department of Chemistry, University of Rochester, Rochester, New York 14627, and Facultad de Química, Universidad Nacional Autónoma de México, México City, México D. F. 04510

Received May 9, 2008

The nickel(0) fragment [Ni(dippe)] was reacted with benzonitrile and initially formed both η^2-nitrile and η^2-arene complexes at −60 °C. When the sample was warmed to room temperature, the latter completely converted to the η^2-nitrile product, which is known to give an equilibrium mixture with the Ni(II) oxidative addition product [(dippe)Ni(Ph)(CN)]. Thermodynamic parameters for this equilibrium have been obtained in both polar and nonpolar solvents (THF vs toluene). Use of density functional theory showed three relatively stable η^2-arene intermediates, as well as six well-defined transition states located on the potential energy surface between the η^2-nitrile complex and the C−CN bond activation product. Among these transition states, those for the migration of the nickel metal between the carbon−carbon bonds of the phenyl ring are at lower energies than those connecting the η^2-nitrile complex to the η^2-arene intermediate and the η^2-arene intermediate to the C−CN bond activation product. Calculations were carried out both in the gas phase and in solution using the PCM model, which was critical for simulation of the different polar solvent environments in these experiments.

Introduction

Carbon−carbon bond activation is attracting increased interest in chemistry because this reaction has a broad range of applications. For example, breaking the C−C bond in alkanes can lead to skeletal rearrangement or cracking, which are important in industrial petroleum refining.[1] The transition metal catalyzed activation of C−C bonds has been used in organic synthesis, for which the beneficial features of atom economy and chemoselectivity have been highlighted.[2] However, the target carbon−carbon σ-bond is both strong and kinetically inert, which makes its cleavage under mild homogeneous conditions a fundamental challenge in organometallic chemistry. The activation is primarily limited to systems in which relief of strain or aromatization serves as a driving force.[3]

A notable exception to this is the oxidative addition of unstrained C−CN bonds of nitriles without neighboring coordinating groups,[4] which can lead to the selective functionalization of organic nitriles.[5] The scission of the C−CN bond of acetonitrile has been reported by Brookhart using a known alkane and arene C−H activation fragment, [Cp*Rh(PMe_3)], along with the use of silanes.[6] The same kind of cleavage has also been achieved by photolysis of the *ansa*-molybdenocene [$Me_2Si(C_5Me_4)_2$]MoH_2 and silyl iron complex $Cp(CO)_2Fe(SiMe_3)$[7] in acetonitrile. Our group has investigated the reactions of aromatic, allylic, and alkyl nitriles using [(dippe)NiH]$_2$.[8] These studies demonstrated that [(dippe)Ni(η^2-NCR)] was initially generated followed by C−C bond cleavage. An interesting result is that, in the reaction of [(dippe)NiH]$_2$ with benzonitrile, (dippe)Ni(η^2-NCPh) undergoes reversible insertion of nickel into the Ph−CN bond, resulting in an equilibrium mixture of Ni(II) and Ni(0) adducts.

In this paper, we report the results of low-temperature activation of benzonitrile with the [Ni(dippe)] fragment and also the thermodynamic results in different solvents. DFT calculations incorporating solvent were conducted on [Ni(dmpe)] as a model for the [Ni(dippe)] fragment, to examine the energetics, possible reaction intermediates, and reaction pathways leading to the C−CN oxidative addition product. Three important

* Corresponding author. E-mail: jones@chem.rochester.edu.

(1) Crabtree, R. H. *Chem. Rev.* **1985**, *85*, 245–269.

(2) (a) Dyker, G. *Angew. Chem.* **1999**, *111*, 1808;*Angew. Chem., Int. Ed.* **1999**, *38*, 1698. (b) Shilov, A. E.; Shul'pin, G. B. *Chem. Rev.* **1997**, *97*, 2879. (c) Ryabov, A. D. *Chem. Rev.* **1990**, *90*, 403.

(3) (a) Murakami, M.; Ito, Y. In *Topics in Organometallic Chemistry*; Murai, S., Ed.; Springer-Verlag: New York, 1999; pp 97−129. (b) Rybtchinski, B.; Milstein, M. *Angew. Chem., Int. Ed.* **1999**, *38*, 870–883. (c) Perthuisot, C.; Edelbach, B. L.; Zubris, D. L.; Simhai, N.; Iverson, C. N.; Muller, C.; Satoh, T.; Jones, W. D. *J. Mol. Catal. A* **2002**, *189*, 157–168.

(4) (a) Parshall, G. W. *J. Am. Chem. Soc.* **1974**, *96*, 2360. (b) Liu, Q. X.; Xu, F.-B. *Organometallics* **2004**, *23*, 610. (c) Burmeister, J. L.; Edwards, L. M. *J. Chem. Soc. A* **1971**, *1663*. (d) Ozawa, F.; Iri, K.; Yamamoto, A. *Chem. Lett.* **1982**, *1707*. (e) Adam, R.; Villiers, C.; Ephritikhine, M.; Lance, M.; Nierlich, M.; Vigner, J. *J. Organomet. Chem.* **1993**, *445*, 99. (f) Marlin, D. S.; Olmstead, M. M.; Mascharak, P. K. *Angew. Chem., Int. Ed.* **2001**, *40*, 4752. (g) Lu, T.; Zhuang, X.; Li, Y.; Chem, S. *J. Am. Chem. Soc.* **2004**, *126*, 4760.

(5) (a) Miller, J. A. *Tetrahedron Lett.* **2001**, *42*, 6991. (b) Miller, J. A.; Dankwardt, J. W. *Tetrahedron Lett.* **2003**, *44*, 1907. (c) Miller, J. A.; Dankwardt, J. W.; Penney, J. M. *Synthesis* **2003**, *11*, 1643. (d) Penney, J. M.; Miller, J. A. *Tetrahedron Lett.* **2004**, *45*, 4989. (e) Crestani, M. G.; Arevalo, A.; Garcia, J. J. *Adv. Synth Catal.* **2006**, *348*, 732. (f) Crisostomo, C.; Crestani, M. G.; Garcia, J. J. *J. Mol. Catal.* **2007**, *266*, 139. (g) Nakao, Y.; Oda, S.; Hiyama, T. *J. Am. Chem. Soc.* **2004**, *126*, 13904–13905. (h) Nakao, Y.; Hiyama, T. *Jpn. Kokai Tokkyo Koho* **2006**, 19pp. (i) Nakao, Y.; Yada, A.; Satoh, J.; Ebata, S.; Oda, S.; Hiyama, T. *Chem. Lett.* **2006**, *35*, 790. (j) Nakao, Y.; Oda, S.; Yada, A.; Hiyama, T. *Tetrahedron* **2006**, *62*, 7567. (k) Tobisu, M.; Kita, Y.; Chatani, N. *J. Am. Chem. Soc.* **2006**, *128*, 8512.

(6) Taw, F. L.; White, P. S.; Bergman, R. G.; Brookhart, M. *J. Am. Chem. Soc.* **2002**, *124*, 4192.

(7) (a) Churchill, D.; Shin, J. H.; Hascall, T.; Hahn, J. M.; Bridgewater, B. M.; Parkin, G. *Organometallics* **1999**, *18*, 2403. (b) Nakazawa, H.; Kawasaki, T.; Miyoshi, K.; Suresh, C. H.; Koga, N. *Organometallics* **2004**, *23*, 117.

(8) (a) Garcia, J. J.; Arévalo, A.; Brunkan, N. M.; Jones, W. D. *Organometallics* **2004**, *23*, 3997. (b) Garcia, J. J.; Brunkan, N. M.; Jones, W. D. *J. Am. Chem. Soc.* **2002**, *124*, 9547. (c) Garcia, J. J.; Jones, W. D. *Organometallics***2000**, *19*, 5544. Note that the sign of ΔX was in error in refs 8b,c.

10.1021/om800424s CCC: $40.75
Publication on Web 06/28/2008

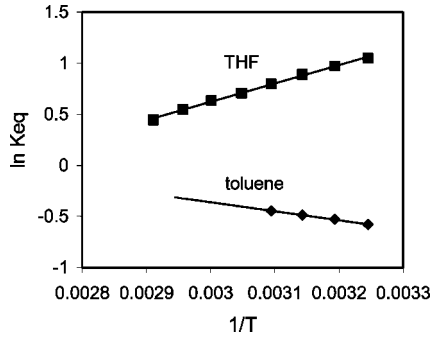

Figure 1. Van't Hoff plot for the equilibrium shown in eq 1 in THF and toluene.

findings are made: (1) the C−C bond being cleaved is *not* in the NiP_2 plane in the C−C cleavage transition state, (2) the two Ni−C bonds are formed before the C−CN bond is broken, and (3) there is a higher energy intermediate involved prior to C−C cleavage: an η^2-arene complex.

Results and Discussion

Thermodynamics of C−CN Cleavage. The reaction of $[Ni(dippe)(\mu\text{-}H)]_2$ with benzonitrile in THF-d_8 solution leads to the rapid formation of the η^2-nitrile complex Ni(dippe)(η^2-NCPh)] (**1**), which equilibrates with the C−CN bond activation product Ni(dippe)(CN)(Ph) (**5**) at ambient temperature over the course of several days (eq 1).[8b] The ratio of **1** to **5** was found to vary with temperature and was determined over the range 35−70 °C. Van't Hoff plots (Figure 1) allowed for the determination of the thermodynamic parameters in both THF ($\Delta H° = -3.57 \pm 0.07$ kcal mol^{-1} and $\Delta S° = -9.5 \pm 0.2$ eu)[8] and toluene ($\Delta H° = 1.75 \pm 0.14$ kcal mol^{-1} and $\Delta S° = 4.5 \pm 0.4$ eu). At 300 K, the formation of [(dippe)Ni(Ph)(CN)] from Ni(0) η^2-CN in THF is slightly downhill ($\Delta G° = -0.72(3)$ kcal mol^{-1}), while in toluene it is uphill ($\Delta G° = 0.39(1)$ kcal mol^{-1}), indicating that differential solvation can effect the thermodynamic preferences of the C−CN cleavage reaction.

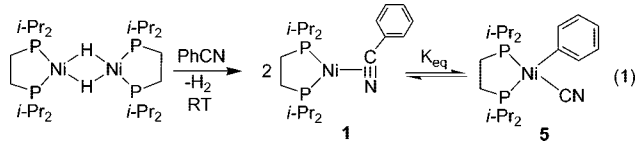

Low-Temperature Reaction of [(dippe)NiH]$_2$ with Benzonitrile. Although in the experiments above no other intermediates were observed, it is possible for nickel to bind to one of the C=C double bonds of the aryl ring, as observed in the case of cyanoquinolines.[8b] These η^2-arene complexes (**2**−**4**) might not be stable at the temperatures at which equilibrium between **1** and **5** is established; therefore, the reaction of $[(dippe)NiH]_2$ with benzonitrile in THF-d_8 was conducted at low temperatures and monitored by NMR spectroscopy. At −60 °C, two sets of signals were observed in the $^{31}P\{^1H\}$ NMR spectrum (Figure 2a). The minor pair of doublets corresponds to those of the previously reported η^2-nitrile complex, **1**. The major resonances in the spectrum appear as two doublets, indicating the presence of two chemically inequivalent phosphines, at δ 53.38 ($^2J_{P-P} = 80$ Hz) and 58.16 ($^2J_{P-P} = 80$ Hz). The ^1H NMR spectrum (Figure 2b) shows three upfield proton resonances at δ 6.72 (1H), 6.90 (2H), and 7.37 (2H), assigned to the para, meta, and ortho protons of an η^2-arene complex. No hydride resonances were observed. The observation of only three signals for the aromatic protons suggests rapid equilibration

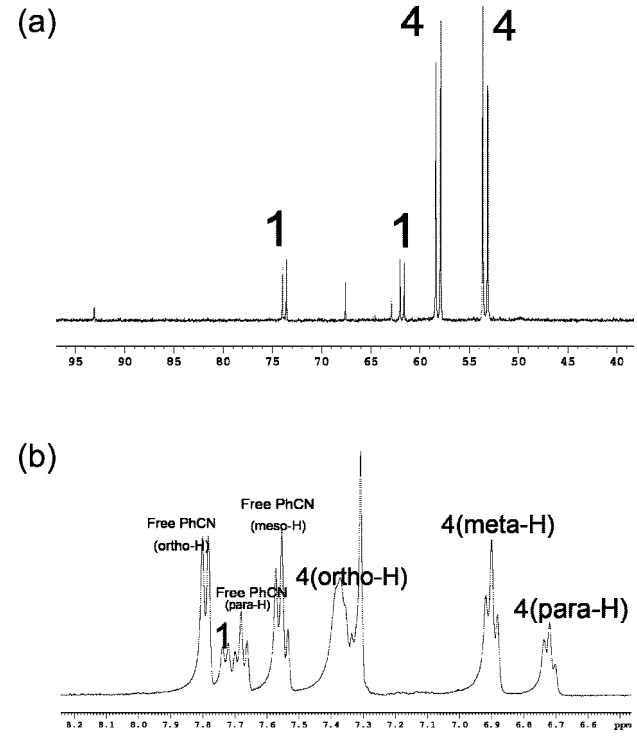

Figure 2. NMR spectra of reaction of $[Ni(dippe)H]_2$ with PhCN at −60 °C (THF-d_8): (a) $^{31}P\{^1H\}$; (b) ^1H.

of isomers (eq 2), and the large upfield shift of the meta and para protons suggests dominant coordination through the double bond between the meta and para carbons as in **4**. Note that while the fluxional process equilibrates the two halves of the ring, it does not equilibrate the two phosphorus environments.[9] The details of such a process will be discussed following computational calculations of the transition states for migration (vide infra). As the temperature of the sample increased, the ratio of the resonances changed, and at 10 °C, the η^2-arene complex completely disappeared, producing only η^2-nitrile complex **1**. When a solution of **1** was cooled to −40 °C, none of the η^2-arene complex was observed to reappear in the ^{31}P NMR spectrum (Supporting Information, Figure SI-1). The possibility that **4** is a T-shaped N-bound benzonitrile complex can be ruled out, as calculations show this species to be symmetrical, not T-shaped (vide infra).

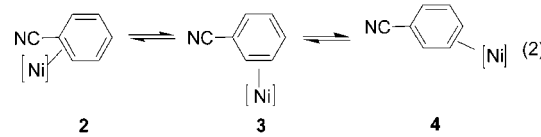

Computational Results: Ground States. On the basis of the observations that the low-temperature reaction of [(dippe)NiH]$_2$ with benzonitrile gave two different nickel(0) complexes, a computational study was undertaken to examine the energetics and reaction pathways leading to the C−CN oxidative addition product from these intermediates. The reaction of the [Ni(dmpe)] fragment with benzonitrile was used as a model, with the methyl groups replacing the isopropyl groups. This simplification is assumed to have no steric outcome on the calculations, as the isopropyl groups of the dippe ligand are

(9) The related complex Ni(dtbpe)(η^2-benzene) has a fluxional NMR spectrum. See: Bach, I.; Pörschke, K. R.; Goddard, R.; Kopiske, C.; Krüger, C.; Rufinska, A.; Seevogel, K. *Organometallics* **1996**, *15*, 4959.

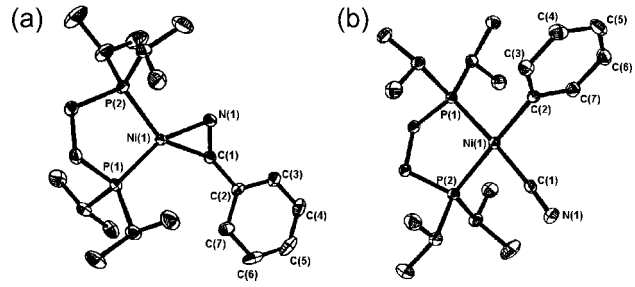

Figure 3. (a) ORTEP drawing of Ni(dippe)(η^2-NCPh) (**1**). Ellipsoids are shown at the 30% level. Selected distances (Å) and angles (deg): N(1)−C(1) = 1.225(6), Ni(1)−N(1) = 1.908(3), Ni(1)−C(1) = 1.867(4), C(1)−C(2) = 1.475(6); N(1)−C(1)−C(2) = 136.1(4). (b) ORTEP drawing of Ni(dippe)(Ph)(CN) (**5**). Ellipsoids are shown at the 30% level. Selected distances (Å) and angles (deg): N(1)−C(1) = 1.148(3), Ni(1)−C(2) = 1.935(2), Ni(1)−C(1) = 1.877(3); C(1)−Ni(1)−C(2) = 89.62(10).

pointing away from the benzonitrile moiety. Sample calculations of **S1**, **S5**, **TS12**, and **TS25** confirm this assumption, showing the dippe complexes to be 1−2 kcal/mol less stable than their dmpe counterparts (see Supporting Information). Initially, local minima for the η^2-nitrile, Ni(dmpe)(η^2-NCPh) (**S1**), and the C−CN oxidative addition product, Ni(dmpe)(Ph)(CN) (**S5**), were found in gas phase calculations, based upon the known X-ray structures for **1** and **3** (Figure 3).[8]

The relative energies of these structures, however, contradicted the experimental observations in that **S5** was found to lie 5.3 kcal mol^{-1} higher in energy than **S1**. This difference was attributed to the high polarity of the C−CN oxidative addition product (dipole moment = 11.1 D) and the lack of inclusion of solvation effects in the gas phase calculations. Therefore, solvent effects on the relative stabilities of all structures were taken into consideration in all further calculations in terms of the polarizable continuum model (PCM).[10] Inclusion of solvation using this model shows **S5** to now lie 0.9 kcal mol^{-1} below **S1**, in excellent agreement with experiment.[11] The optimized structural parameters and relative energies of all stable species and transition states found in this study are summarized in Table 1, Figure 4, and Figure 5. Species **S2**, **S3**, and **S4** represent the three possible η^2-C,C-arene complexes.

Of the optimized structures summarized in Figure 4, only the dippe analogues of the η^2-coordinated nitrile (**S1**) and the C−CN oxidative addition product (**S5**) are stable enough to be isolated experimentally. These optimized structures are highly consistent with their crystallographic data. In **S1**, the coordinated C−N bond is longer than in free benzonitrile (1.23 vs 1.16 Å), and the nitrile group deviates from linearity (the C−C−N angle is 137.8° vs 180°), much in resemblance to actual data of compound **1**. The Ni−P bonds are lengthened relative to [Ni(dmpe)], due to the trans influence of the nitrile ligand. In the X-ray crystal structure of **1**, the coordination around nickel is essentially planar, with the carbon and nitrogen atoms of the nitrile group completing the corners of the square plane. The phenyl group is also coplanar with the Ni1−N1−C1 plane and the square plane of the complex. However, the energy difference between the two structures where the phenyl ring is planar, **S1**, and perpendicular, **S1′**, is only 2.6 kcal mol^{-1}, which is consistent with the observation of free rotation around the C1−C2 bond seen in the ^{1}H NMR spectrum.

The optimized structure of the C−CN bond activation product, **S5**, has the expected square-planar geometry around the metal center. The phenyl ring is now perpendicular to the square plane of the complex. The structure where the phenyl ring is coplanar with the square plane of the complex, **S5′**, is 7.6 kcal mol^{-1} higher in energy than where it is perpendicular; so again free rotation is expected.

The transition state leading to the formation of the C−CN oxidative addition product was located from a relaxed potential energy surface scan[12] by constraining the C−CN distance in **S5** and optimizing the resulting structures as the C−C distance was reduced. The structure around the energy maximum was optimized as a transition state (**TS25**). The intrinsic reaction coordinate calculation (IRC) starting from this transition state connected the oxidative addition product to the η^2-arene complex **S2**, where the nickel metal is coordinated through the C=C between the ipso and ortho carbons of the benzonitrile. When the Ni−CN distance in **S2** was constrained to shorten in a relaxed potential energy surface scan, it also leads to the same transition state that connects it with **S5**.

η^2-Arene Complexes. There are three stable, high-energy η^2-arene species (+12.1, 13.0, and 12.9 kcal mol^{-1} relative to **S1**), **S2**, **S3**, and **S4**. In these structures, nickel metal binds to the phenyl ring through one of the C=C double bonds. The nickel carbon bond lengths (Ni−C_{aryl} = 2.0 Å) are very similar to each other, and the bond lengths between the two carbons coordinated to the nickel are around 1.45 Å. The angle between the phenyl ring and the P−Ni−P plane is at 110.8° in **S2**, 108.5° in **S3**, and 103.8° in **S4**. The transition states connecting these η^2-arene species with each other (**TS23**, **TS34**) were also located by relaxed potential energy surface scans. These transition states show an η^3-allyl-like structure with the allyl perpendicular to the P−Ni−P plane and are at lower energies than those connecting the η^2-nitrile to the η^2-arene or the η^2-arene to the oxidative addition product (**TS12**, **TS25**).

The transition state **TS22**, which is 7.9 kcal mol^{-1} higher in energy than **S2**, represents the barrier for the migration of the nickel metal from one ortho carbon to the other ortho carbon. Through the transition states **TS23** and **TS34**, nickel migrates from the ipso carbon to the meta carbon and the ortho carbon to the para carbon, respectively. **TS44** is the transition state for migration of the nickel fragment from one meta carbon to the other meta carbon. The energies of all these transition states are lower than the C−CN bond activation barrier. Note that as a result of the perpendicular orientation of the allyl-like transition states, the two phosphorus atoms maintain distinct environments and do not interchange. The NiP_2 unit effectively "twirls" as it migrates to preserve these distinct environments (see movie in Supporting Information). A simpler "slipping" of the Ni(dippe) unit around the ring would equilibrate phosphorus environments. The observation of equilibrating proton but distinct phosphorus environments provides experimental validation of these calculated transition states and the mechanism of fluxionality.

The low kinetic barriers for the migration of the nickel around the phenyl ring hinder the detection of the different η^2-arene species in the NMR spectrum even at −60 °C. The small thermodynamic driving force favoring the C−CN bond activation product over the η^2-nitrile complex is fully consistent with

(10) This model "rolls" a spherical dipole of the same size and magnitude as THF over the surface of the molecule to account for solvent−solute interactions. See: Miertus, S.; Scrocco, E.; Tomasi, J. *Chem. Phys.* **1981**, *55*, 117.

(11) In addition, PCM correction of the two species in toluene shows the conversion of **S1** to **S5** to still be uphill by 1.9 kcal mol^{-1}. See the Supporting Information for the energies of all species in toluene.

(12) Foresman, J. B.; FrischÆ. *Exploring Chemistry with Electronic Structure Methods*, 2nd ed.; Gaussian, Inc.: Pittsburgh, 1996; pp 171−172.

Table 1. Optimized Structures (interatomic distances in Å, angles in deg) and Relative Free Energies (ΔG, kcal mol^{-1}) of Stationary Points on the [Ni(dmpe)] + PhCN Potential Energy Surface (PCM corrected in THF)

	Ni−C_{ipso}	Ni−C_{ortho}	Ni−C_{meta}	Ni−C_{para}	Ni−CN	Ni−N	C−CN	C−N	N−C−C_{α}	α	ΔG
S1	3.228				1.874	1.902	1.466	1.234	137.8	1.04[a]/2.93[b]	−31.24
S1′	3.195				1.879		1.464	1.230	142.0	2.16[a]/84.91[b]	−28.60
TS12	2.422				2.028		1.431	1.184	173.5	68.37[c]	−1.04
S2	2.004	1.993			2.715		1.436	1.168	178.1	110.84[b]	−19.16
TS22	1.946	2.320			2.821		1.435	1.167	179.0	89.55[b]	−11.30
TS23	2.310	1.940	2.329		3.067		1.432	1.166	178.6	82.60[b]	−10.10
S3		1.985	2.010				1.429	1.166	177.3	108.51[b]	−18.23
TS34		2.314	1.961	2.295			1.433	1.165	179.8	89.57[b]	−9.41
S4			2.014	2.001			1.429	1.166	179.5	103.78[b]	−18.35
TS44			2.326	1.960			1.424	1.167	179.7	88.66[b]	−13.32
TS25	2.033				1.874	2.418	1.590	1.189	139.9	27.85[c]	−2.03
S5	1.926				1.867		2.733	1.171	143.2	88.61[b]	−32.12
S5′	1.967				1.867		2.799	1.172	144.0	10.24[b]	−24.47

[a] Angle between P−Ni−P and Ni−C≡N planes. [b] Angle between P−Ni−P and phenyl planes. [c] Angle between C_{aryl}−Ni−CN and P−Ni−P planes.

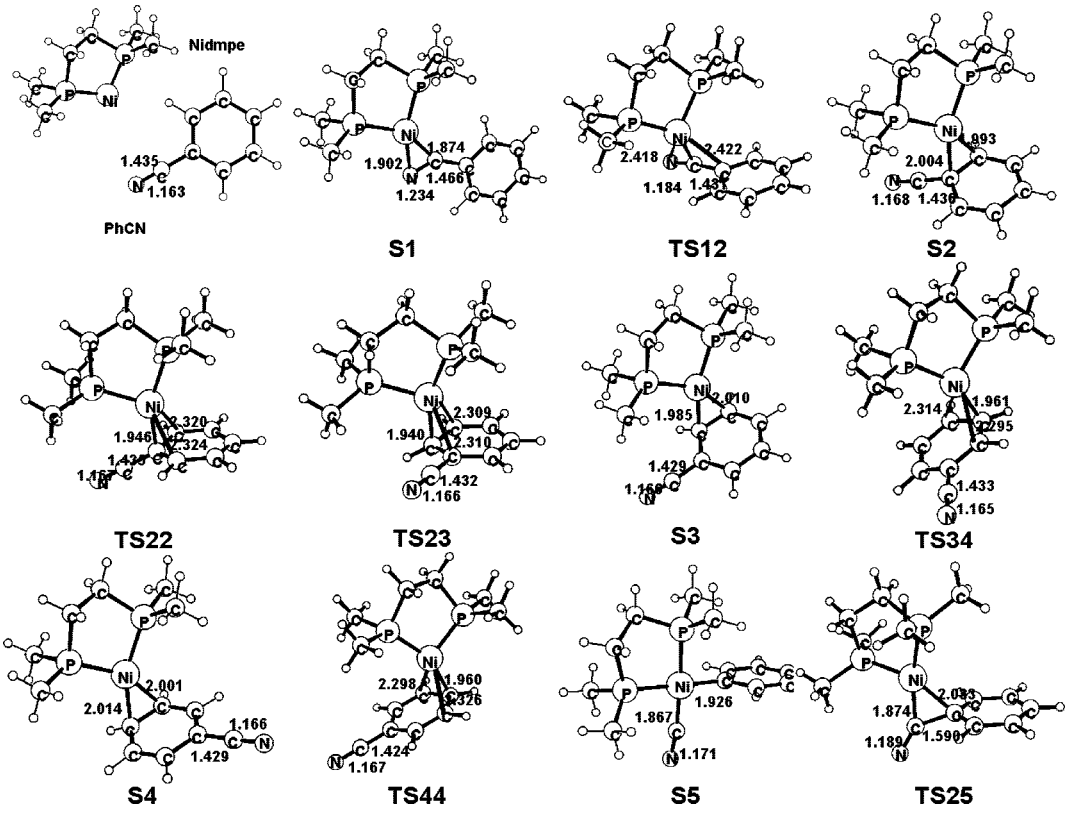

Figure 4. Optimized structures (interatomic distances in Å, angles in deg) of stationary points and transition states on the [Ni(dmpe)] + PhCN potential energy surface.

the experimental observation of equilibrium between these two species in THF.

It is interesting to note that this same type of migration of a Ni($H_2PCH_2CH_2PH_2$) fragment around the double bonds of perfluorobenzene has been calculated by McGrady and Perutz.[13] The perpendicular geometry in the transition state to migration was also noted. It is also worth commenting that this twirling migration of the NiP_2 fragment corresponds to the "retention" motion predicted for the orbitally allowed degenerate sigmatropic shifts in norcaradiene.[14] Ironically, however, norcaradiene rearrangements have been shown experimentally[15] and theoretically[16]to proceed via the orbitally forbidden "inversion" pathway. We have also calculated a transition state for migration around the benzonitrile arene ring via an inversion pathway (which corresponds to a geometry with the η^3-arene parallel to the NiP_2 plane), and it lies ∼8 kcal/mol higher in energy than the retention pathway (see Supporting Information, Figure SI-4).

Another possible binding mode of the benzonitrile would be η^1-N-bound. The geometry of this species was optimized, showing a C_2-symmetrical structure (see Supporting Information). The free energy (w/PCM in THF) was found to be −18.7 kcal/mol relative to the free fragments, comparable to the η^2-arene complex energies. However, no evidence for such a species is seen by low-temperature NMR spectroscopy.

(13) Reinhold, M.; McGrady, J. E.; Perutz, R. N. *J. Am. Chem. Soc.* **2004**, *126*, 5268.

(14) Berson, J. A. *Acc. Chem. Res.* **1968**, *1*, 152.

(15) (a) Klärner, F.-G. *Angew. Chem., Int. Ed. Engl.* **1974**, *13*, 268. (b) Klärner, F.-G.; Brassel, B. *J. Am. Chem. Soc.* **1980**, *102*, 2469. (c) Baldwin, J. E.; Broline, B. M. *J. Am. Chem. Soc.* **1982**, *104*, 2857. (d) Baldwin, J. E.; Broline, B. M. *J. Org. Chem.* **1982**, *47*, 1385.

(16) (a) Schoeller, W. W. *J. Am. Chem. Soc.* **1975**, *97*, 1978. (b) Kless, A.; Nendel, M.; Wilsey, S.; Houk, K. N. *J. Am. Chem. Soc.* **1999**, *121*, 4524.

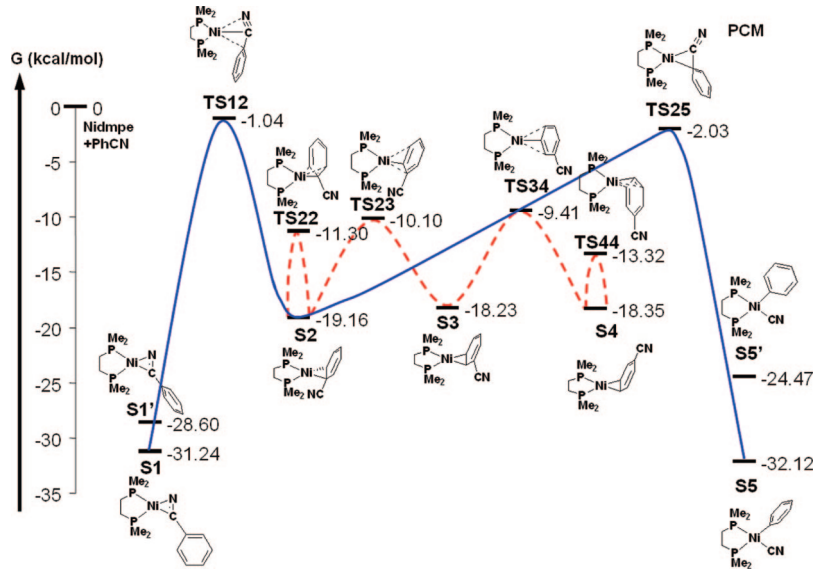

Figure 5. Energetics of C−C bond activation of benzonitrile by [Ni(dmpe)] (free energies in kcal mol^{-1}) relative to the total energies of fragments ([Ni(dmpe)] and PhCN) (PCM corrected in THF).

Relation of η^2-CN to η^2-Arene Complex. The unstable η^2-arene intermediate, **S2**, lies at the center of the reactivity in this system. The transition state, **TS12**, was located by constraining the distance between Ni and C_{ipso} from 3.23 to 1.92 Å by six steps. It connects the η^2-coordinated nitrile **S1** to the η^2-coordinated arene intermediate **S2**. The connections of **TS12** were confirmed by an intrinsic reaction coordinate calculation starting from **TS12**, which is 30.2 kcal mol^{-1} higher in energy than **S1**. The nitrile in **TS12** coordinates to the nickel center through the nitrile carbon (Ni−CN = 2.03 Å) and, more weakly, through its nitrogen and aryl carbon atoms (Ni−N = 2.42 Å, Ni−C_{ipso} = 2.42 Å). The plane defined by these three atoms, Ni−C−N, is at an angle of 62.2° to the P−Ni−P plane. **S2** corresponds to an η^2-arene complex in which nickel metal is coordinated to the benzonitrile through the C_{ipso}=C_{ortho} double bond and is 18.1 kcal mol^{-1} lower in energy than **TS12**. Motion along the reaction coordinate at **TS12** looks like a rocking motion, in which the aryl ortho-carbon or η^2-nitrile alternately approaches the metal.

As mentioned above, transition state **TS25** leading to the C−CN bond cleavage product connects **S5** to **S2** and was located 17.1 kcal mol^{-1} higher in energy than **S2** and 30.1 kcal mol^{-1} higher in energy than **S5**. In **TS25**, the C−CN bond is 0.15 Å longer than that in **S2**, and the C−C−N angle is 139.9°, much smaller than in **S2** (178.1°). The ipso carbon moves to 2.03 Å from nickel, close to its target value of 1.93 Å in **S5**. The cyano carbon is only 1.87 Å from nickel, which is 0.007 Å longer than in the product **S5**. Also, the C_{ipso}−Ni−C(N) plane has now rotated to an angle of 27.8° to the P−Ni−P plane. The C−C bond is lengthened to 1.59 Å. Consequently, the C−C bond cleavage transition state can be viewed as having essentially formed the two new Ni−C bonds while only slightly breaking the C−CN bond and is well-progressed toward the nickel(II) square-planar product geometry. It is interesting to note that in the **S2** → **TS25** → **S5** conversion the arene rotates about its normal by 120° relative to the NiP_2 plane (eq 3).

The relationships among ground states, η^2-arene complex, and transition states can also be seen on the potential energy surface shown in Figure 6. The scan of the potential energy surface (gas phase) was carried out by varying the distance between the ipso carbon and the nitrile carbon (d_{C-CN}) and that between nickel and the ipso carbon ($d_{Ni-Cipso}$). There are three

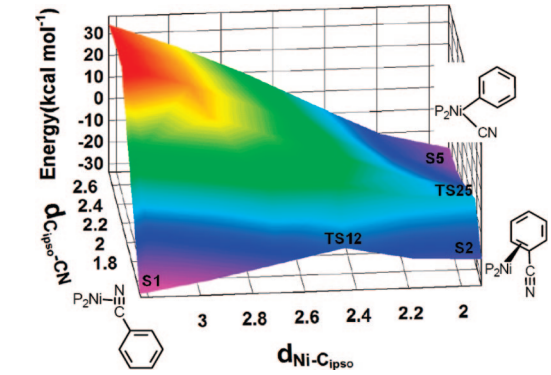

Figure 6. Potential energy surface of complexes **S1**−**S5** (gas phase).

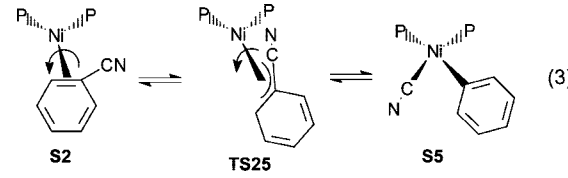

local minima corresponding to the η^2-nitrile (**S1**), η^2-arene (**S2**), and C−CN bond activation product (**S5**). Two saddle points were located corresponding to the transition state connecting **S1** to **S2** (**TS12**) and that connecting **S2** to **S5** (**TS25**). There is no direct pathway connecting **S1** to **S5**.

The energy barrier in Figure 5 between **S2** and **TS25** is lower than that between **S2** and **TS12** by 1.0 kcal mol^{-1}, which should make it possible for **S2** to convert to both **S1** and **S5**. However, it is observed experimentally that **S1** was formed immediately after mixing the reagents, while **S5** was observed only over several days. One reason for this discrepancy might be that the Ni(dmpe) fragment used in the calculations has less steric hindrance when nickel binds to benzonitrile compared to the Ni(dippe) fragment used in the experiment. The angle between C−C−N and the P−Ni−P plane in **TS12** is 75.0° and that in **TS25** is 33.5°. Thus the phenyl ring of **TS25** is closer to the methyl group than that of **TS12**. In the "real" reaction between [Ni(dippe)] and PhCN, the isopropyl group would destabilize **TS25** more than **TS12**, so the energy of **TS25** might be higher

than **TS12**, which would result in the preferential formation of **S1** over **S5** from **S2**. However, DFT calculations on the full Ni(dippe) system show that **TS25** is still lower in energy than **TS12** (see Supporting Information, Figures SI-2,3). Consequently, it appears that this level of calculation cannot predict kinetic selectivity when the barriers are so close in energy. In examination of the energetics of **S1** and **S2** in Figure 5, no **S2** should be seen in equilibrium with **S1**, as observed experimentally.

Finally, it is worth comparing the conversion of **S1** to **S5** via **TS25** with the C−CN cleavage of acetonitrile in Ni(dippe)(η^2-$NCCH_3$), reported earlier.[17] In the case of acetonitrile, the η^2-nitrile complex was found (via DFT calculations) to convert first to a stable η^3-C,C,H (agostic C−H) complex prior to cleavage of the C−CN bond. In this species, the η^3-ligand was perpendicular to the NiP_2 plane, showing a similar geometry to the η^3-arene species discussed above for benzonitrile fluxionality in **2**, **3**, and **4**. Likewise, in the C−CN cleavage transition state for acetonitrile, the C−CN bond is virtually intact, while the Ni−CH_3 and Ni−CN bonds are almost completely formed, as seen with benzonitrile. In addition, the C−C bond being cleaved was at an angle of 39° to the NiP_2 plane, comparable to the angle of 28° seen with benzonitrile here. Consequently, these two C−CN cleavage reactions appear to have much in common with each other in terms of the immediate precursor geometry to C−CN cleavage, despite the fact that one involves sp−sp^2 bond cleavage and the other sp−sp^3 bond cleavage.

Conclusions

The reaction of $[(dippe)NiH]_2$ with benzonitrile at low temperature leads to the formation of both η^2-nitrile and η^2-arene complexes. According to the DFT calculations using [Ni(dmpe)] as a model of [Ni(dippe)], the total free energy of the η^2-nitrile complex in THF solution is found to be ∼12 kcal mol^{-1} lower than that of the η^2-arene complexes. This matches the experimental observations in that at ambient temperatures the latter is converted to the former. Due to the high polarity of the C−CN bond cleavage product, solvent effects were taken into consideration in all DFT calculations in terms of the PCM correction in order to achieve good agreement with experiment. The transition states were located on the potential energy surface for the stepwise migration of the nickel from the η^2-nitrile to the adjacent double bond of the arene and for fluxionality around the phenyl ring. This fluxionality follows an orbitally allowed "retention" pathway for migration. The transition state for the C−CN cleavage was found to connect with the η^2-arene complex in which the cyano group is attached to the bound double bond. The transition state **TS25** indicates that substantial bond making occurs prior to C−CN bond cleavage and is at an angle of ∼30° to the NiP_2 plane.

Experimental Section

General Procedures. All reactions were carried out using standard Schlenk and glovebox techniques, under nitrogen. Solvents were dried and distilled before use from sodium/benzophenone ketyl. Also, deuterated solvents (Cambridge Isotope Laboratories) for NMR experiments were dried over sodium/benzophenone ketyl and distilled under vacuum. All other chemicals and filter aids were reagent grade and were used as received. ^1H and $^{31}P\{^1H\}$ NMR spectra were determined on AVANCE400 or AVANCE500 spectrometers in THF-d_8 or toluene-d_8; chemical shifts (δ) are relative to the deuterated solvent residual protons, and $^{31}P\{^1H\}$ NMR spectra are relative to external 85% H_3PO_4. The synthesis of $[Ni(dippe)H]_2$ was carried out using the reported procedure.[18] Benzonitrile was purchased from Aldrich and distilled before use.

Computational Details. When available, known experimental structures for the complexes were used as the starting point for the calculations. To simplify these calculations, the *i*-Pr groups were substituted by methyl groups (see Supporting Information for sample calculations with Ni(dippe)). The gas phase structures were fully optimized in redundant internal coordinates,[19] with density-functional theory (DFT) and a wave function incorporating Becke's three-parameter hybrid functional (B3),[20] along with the Lee−Yang−Parr correlation functional (LYP).[21] All calculations were performed using the Gaussian03[22] package. The Ni and P atoms were represented with the effective core pseudopotentials of the Stuttgart group and the associated basis sets improved with a set of f-polarization functions for Ni ($\alpha = 3.130$)[23] and a set of d-polarization functions for P ($\alpha = 0.387$).[24] The remaining atoms (C, H, and N) were represented with 6-31G(d,p)[25] basis sets. The geometry optimizations were performed without any symmetry constraints, and the local minima and the transition states were checked by frequency calculations. For each transition-state structure, the intrinsic reaction coordinate (IRC) routes were calculated in both directions toward the corresponding minima. For some of the transition states, the IRC calculations failed to reach the energy minima on the potential energy surface; therefore, in those cases geometry optimizations were carried out as a continuation of the IRC path. Because of the polarity of the structures, the solvent effects on their relative stabilities were evaluated by calculating the free energies of solvation in terms of the polarizable continuum model.[9] The self-consistent reaction field (SCRF) calculations using the PCM-UA0 solvation model[26] were carried out for the gas-phase-optimized structures. The dielectric constant in the PCM calculations was set to $\varepsilon = 7.58$ to simulate THF as the solvent medium used in the experimental study. The energies discussed in the potential energy surface scan are electronic energies without ZPE corrections. Gibbs free energies have been calculated at 298.15 K and 1 atm. The Ortep32 package was used to display the molecular structures.

Thermodynamic Equilibration of 1 and 5 in THF-d_8. $[Ni(dippe)H]_2$ (32.9 mg, 0.051 mmol) and benzonitrile (10.5 μL, 0.102 mmol) were mixed in THF-d_8 (0.6 mL) in an NMR tube. The mixture turned golden brown immediately, and H_2 gas was evolved. The tube was placed in an oil bath at a regulated temperature, and the conversion of the Ni(0) to the Ni(II) was monitored periodically by $^{31}P\{^1H\}$ NMR spectroscopy until an equilibrium mixture of the two was obtained. $K_{eq} = [Ni(II)]/[Ni(0)]$ was calculated from the integrations of $^{31}P\{^1H\}$ NMR spectra of the equilibrium mixture with inverse-gated ^1H decoupling.

Thermodynamic Equilibration in Toluene-d_8. $[Ni(dippe)H]_2$ (18.9 mg, 0.029 mmol) was mixed with benzonitrile (6.4 μL, 0.062 mmol) in toluene-d_8 (0.5 mL). The same procedure was carried out as above.

Low-Temperature Reaction of $[Ni(dippe)H]_2$ with Benzonitrile. $[Ni(dippe)H]_2$ (10 mg, 0.016 mmol) was dissolved in THF-d_8, transferred into an NMR tube capped with a septum, and cooled to −78 °C in a dry ice/acetone bath. Then benzonitrile (3.2 μL,

(17) Ateşin, T. A.; Li, T.; Brennessel, W. W.; Lachaize, S.; Garcı´a, J. J.; Jones, W. D. *J. Am. Chem. Soc.* **2007**, *129*, 7562.

(18) Vicic, D. A.; Jones, W. D. *J. Am. Chem. Soc.* **1997**, *119*, 10855.

(19) Peng, C.; Ayala, P. Y.; Schlegel, H. B.; Frisch, M. J. *J. Comput. Chem.* **1996**, *17*, 49.

(20) Becke, A. D. *J. Chem. Phys.* **1993**, *98*, 5648.

(21) Lee, C.; Yang, W.; Parr, R. G. *Phys. Rev. B* **1988**, *37*, 785.

(22) Frisch, M. J., *Gaussian03*; Gaussian, Inc.: Wallingford, CT, 2004.

(23) Ehlers, A. W.; Bohme, M.; Dapprich, S.; Gobbi, A.; Hollwarth, A.; Jonas, V.; Kohler, K. F.; Stegmann, R.; Veldkamp, A.; Frenking, G. *Chem. Phys. Lett.* **1993**, *208*, 111.

(24) Hollwarth, A.; Bohme, M.; Dapprich, S.; Ehlers, A. W.; Gobbi, A.; Jonas, V.; Kohler, K. F.; Stegmann, R.; Veldkamp, A.; Frenking, G. *Chem. Phys. Lett.* **1993**, *208*, 237.

(25) Hehre, W. J.; Ditchfield, R.; Pople, J. A. *J. Chem. Phys.* **1972**, *56*, 2257.

0.031 mmol, dissolved in 0.02 mL of THF) was added while the tube was still in the dry ice/acetone bath. ^{1}H and ^{31}P{^{1}H} NMR spectra were recorded once every 10 °C as the reaction mixture was warmed from −60 to 60 °C in the NMR probe. NMR spectra for **S4** in THF-d_8 (−60 °C), ^{1}H: δ 6.72 (t, $^{2}J_{P-H}$ = 7 Hz, 1H, para-H), 6.90 (t, $^{2}J_{P-H}$ = 7 Hz, 2H, meta-H), 7.37 (s, br, 2H, ortho-H), ^{31}P{^{1}H}: δ 53.38 (d, $^{2}J_{P-P}$ = 80 Hz), 58.16 (d, $^{2}J_{P-P}$ = 80 Hz). NMR spectra for **S1** in THF-d_8 (−60 °C), ^{31}P{^{1}H}: δ 61.83 (d,$^{2}J_{P-P}$ = 66 Hz), 73.77 (d, $^{2}J_{P-P}$ = 66 Hz).

Acknowledgment is made to the U.S. Department of Energy for financial support for Ting Li (grant FG02-86ER13569) and the NSF for financial support for Tülay A. Ateşin (grant CHE-0717040).

Supporting Information Available: Complete ref 22. ^{1}H and ^{31}P NMR spectra at variable temperatures, experimental equilibrium parameters for van't Hoff plot, input files for the DFT calculations together with the optimized geometries of the structures, calculated thermodynamic parameters for compounds with PCM correction in toluene and THF, free energies of full (dippe)Ni complexes **S1**, **TS12**, **S2**, **TS25**, and **S5**, transition states for migration with retention and inversion, optimized structure of (dmpe)Ni(η^{1}-NCPh), and a movie file for the fluxional process of **2**, **3**, and **4**. This material is available free of charge via the Internet at http://pubs.acs.org.

OM800424S

(26) Barone, V.; Cossi, M.; Tomasi, J. *J. Chem. Phys.* **1997**, *107*, 3210.